Published in final edited form as:
Neurobiol Aging. 2011 September ; 32(9): 1693–1706. doi:10.1016/j.neurobiolaging.2009.10.001.

Aging-related changes in calcium binding proteins in rat perirhinal cortex

James R. Moyer Jr[a,1,*], **Sharon C. Furtak**[a,2], **John P. McGann**[a,3], and **Thomas H. Brown**[a,b,*]
[a]Department of Psychology, Yale University, New Haven, CT 06520

[b]Department of Cellular and Molecular Physiology, Yale University, New Haven, CT 06520

Abstract

Dysregulation of intracellular calcium homeostasis has been linked to neuropathological symptoms observed in aging and age-related disease. Alterations in the distribution and relative frequency of calcium-binding proteins (CaBPs), which are important in regulating intracellular calcium levels, may contribute to disruption of calcium homeostasis. Here we examined the laminar distribution of three CaBPs in rat perirhinal cortex (PR) as a function of aging. Calbindin-D28k (CB), parvalbumin (PV), and calretinin (CR) were compared in adult (4 mo.), middle-aged (13 mo.) and aged (26 mo.) rats. Results show an aging-related and layer-specific decrease in the number of CB-immunoreactive (-ir) neurons, beginning in middle-aged animals. Dual labeling suggests that the age-related decrease in CB reflects a decrease in neurons that are not immunoreactive for the inhibitory neurotransmitter GABA. In contrast, no aging-related differences in PV- or CR-immunoreactivity were observed. These data suggest that selective alterations in CB-ir neurons may contribute to aging-related learning and memory deficits in tasks that depend upon PR circuitry.

Keywords

calbindin; parvalbumin; calretinin; immunohistochemistry; laminar distribution; medial temporal lobe; middle-aged; aged

1. Introduction

According to the calcium hypothesis of aging (Khachaturian, 1987, 1994; Landfield, 1987), dysregulation of intracellular calcium ($[Ca^{2+}]_i$) homeostasis is a primary factor contributing to aging-related learning and memory impairments in humans and other mammals. Animal

[1]Present address of Dr. James R. Moyer, Jr., Department of Psychology, University of Wisconsin-Milwaukee, Milwaukee, WI 53201.
[2]Present address of Dr. Sharon C. Furtak, Department of Psychology, Brown University, Providence, RI 02912.
[3]Present address of Dr. John P. McGann is Department of Psychology, Rutgers University, Piscataway, NJ 08854.
[*]**Corresponding authors**:
Dr. James R. Moyer, Jr.; Department of Psychology, P.O. Box 413, University of Wisconsin-Milwaukee, Milwaukee, WI 53201; Tel: (414) 229-3255; jrmoyer@uwm.edu
Dr. Thomas H. Brown; Department of Psychology, 2 Hillhouse Ave., Yale University, New Haven, CT 06520; Tel: (203) 432-7326; thomas.brown@yale.edu

Disclosure Statement: There are no real or perceived conflicts of interest.

studies have shown that dysregulation of intracellular calcium homeostasis can lead to excitotoxicity and cell death (Choi, 1992, 1994). In hippocampal neurons, aging-related increases in Ca^{2+}-dependent membrane potentials can be acutely reversed by compounds that block Ca^{2+} influx through L-type Ca^{2+} channels (Moyer and Disterhoft, 1994; Moyer et al., 1992; Thibault et al., 1998). These same compounds also improve associative learning in certain tasks in aged animals (Deyo et al., 1989; Disterhoft et al., 1993; Veng et al., 2003). A number of cellular changes could theoretically contribute to Ca^{2+} dysregulation during aging, including changes in voltage-dependent ion channels (Campbell et al., 1996; Foster, 2007; Thibault et al., 2001; Thibault and Landfield, 1996; Veng et al., 2003), mitochondrial changes (Babcock et al., 1997; Kruman and Mattson, 1999; LaFrance et al., 2005; Leslie et al., 1985; Nicholls, 1985), and changes in Ca^{2+} binding proteins or CaBPs (Amenta et al., 1994; Bu et al., 2003).

The present study examines aging-related changes in three CaBPs—calbindin-D28k (CB), parvalbumin (PV), and calretinin (CR)—that are thought to play an important role in buffering excess intracellular Ca^{2+} (Baimbridge et al., 1992). All three of these CaBPs belong to the same superfamily of E-F hand domain proteins (Heizmann, 1988; Yap et al., 1999). In the brain, they are mostly found in non-overlapping populations of GABAergic interneurons as well as in some pyramidal neurons (e.g., see Andressen et al., 1993; Mikkonen et al., 1997; van Brederode et al., 1991; Van Brederode et al., 1990). Importantly, CaBPs have been implicated in neurodegenerative diseases and impaired memory function. For example, a reduction in CaBPs has been reported in humans diagnosed with Alzheimer's disease (AD, Mikkonen et al., 1999; Mikkonen et al., 1997). Furthermore, calbindin-deficient transgenic mice are impaired on spatial-learning tasks and they fail to maintain long-term potentiation (Molinari et al., 1996), which is a leading candidate synaptic substrate for memory formation (Brown et al., 2004; Brown et al., 2008).

Immunohistochemical methods were used here to investigate the laminar distribution, frequency, and morphology of neurons that are immunoreactive for CB, PV, and CR. The specific focus was on perirhinal cortex (PR), partly because this is one of the first brain regions to show neurodegeneration in Alzheimer's disease (Braak and Braak, 1994, 1995; Detoledo-Morrell et al., 1997; Dickerson et al., 2009; Juottonen et al., 1998; Van Hoesen and Solodkin, 1994) and also because PR is well known to play a critical role in cognitive and emotional aspects of learning (Bang and Brown, 2009; Barker et al., 2007; Bucci et al., 2000; Buckley and Gaffan, 1998a, 1998b; Buffalo et al., 2006; Bussey et al., 2002; Eacott and Norman, 2004; Eichenbaum et al., 2007; Furtak et al., 2007a; Hannesson et al., 2004; Holdstock et al., 2000; Kholodar-Smith et al., 2008; Lindquist et al., 2004; Liu and Bilkey, 1998; Meunier et al., 1993; Murray et al., 2007; Parsana and Brown, in press; Squire et al., 2007; Zola-Morgan et al., 1993). Understanding aging-related changes in CaBPs in animal models may furnish insights into methods for minimizing neurodegeneration in humans.

2. Methods

2.1 Subjects

All experiments involved experimentally naïve male Sprague-Dawley (SD) rats (Charles River, Kingston, NY). Rats were housed individually on a 12-hr day-night cycle (lights on at 7 a.m.), with free access to food and water. All procedures were carried out in strict compliance with both National Institutes of Health and Yale Animal Resource Center guidelines.

For the CB studies, 30 male SD rats (10 young, 10 middle-aged, 10 aged) were used as subjects (mean age ± SD: young 4.3 ± 0.9 months, middle-aged 14.0 ± 2.7 months, aged 27.3 ± 2.4 months). Six of these rats (2 per age group) were used for the double-labeling

studies described below. For the PV studies, 18 male SD rats (6 young, 6 middle-aged, 6 aged) were used as subjects (mean age ± SD: young 4.2 ± 1.6 months, middle-aged 13.2 ± 0.5 months, aged 27.0 ± 4.0 months). For the CR studies, 9 male SD rats (3 young, 3 middle-aged, 3 aged) were used as subjects (mean age ± SD: young 4.8 ± 0.5 months, middle-aged 16.5 ± 0.9 months, aged 31.5 ± 3.7 months).

Rats were anesthetized with halothane followed by either Nembutal (80–90 mg/kg, i.p.) or a combination of ketamine (100 mg/kg, i.p.) and xylazine (20 mg/kg, i.p.). Subjects were perfused through the ascending aorta with 0.9% saline in 0.1 M phosphate buffered saline (PBS) followed by a solution of 4% paraformaldehyde in PBS. The brain was carefully removed and incubated in 4% paraformaldehyde in PBS at 4°C for 24 to 48 hr. Brains were then transferred to a 30% sucrose / PBS solution for at least two days (until the brain sank to the bottom of the container). Brains were then blocked and horizontal sections (50 μm) were cut using a freezing microtome. Sections were then placed into individual wells containing PBS and processed as described below.

2.2 Immunohistochemistry

Procedures for calbindin, parvalbumin, and calretinin labeling—Horizontal sections containing PR were selected for staining. PR was defined according to the coordinates of Burwell and colleagues (Burwell, 2001; Burwell and Amaral, 1998; Burwell et al., 1995; Furtak et al., 2007c). Sections were limited to those corresponding to plates 98 through 100 of a rat stereotaxic atlas (Paxinos and Watson, 1998). Observations were restricted to the rostro-caudal area of PR that is approximately −3.6 to −5.2 mm relative to Bregma (Furtak et al., 2007b), a region that is unequivocally within PR (see Fig. 1).

Free-floating sections were incubated in 1% sodium borohydride ($NaBH_4$) in PBS for 15 min, washed for 10 min in PBS, and incubated for 30 min in a solution of 10% normal goat serum (NGS; Sigma, St. Louis, MO, USA) in PBS. Slices were then incubated in either the primary anti-calbindin antibody (1:1000; mouse, monoclonal, C9848, Sigma), the primary anti-parvalbumin antibody (1:1000; mouse, monoclonal, P3088, Sigma), or the primary anti-calretinin antibody (1:1000; mouse, monoclonal, MAB1568, Chemicon International, Inc., Temecula, CA, USA) in PBS (with 0.2% Triton-X 100 and 3% NGS) overnight at 4°C.

Following primary antibody incubation, the slices were subjected to three consecutive 10 min washes in a solution of PBS/0.2% Triton-X 100. Sections were then incubated in the biotinylated secondary antibody (1:200; goat anti-mouse, Sigma) in a PBS/0.2% Triton-X 100 solution for 1h, followed by three 10 min washes in the PBS/0.2% Triton-X 100 solution. The slices were then incubated in an avidin-HRP ABC solution (Vector Elite ABC Kit; Vector Laboratories, Burlingame, CA, USA) for 2h, followed by three 10 min washes in PBS/0.2% Triton-X 100 solution. Control slices were processed as described except that primary antibody was excluded. Nonspecific staining was not observed. For each reaction, tissue sections from an adult, middle-aged, and aged animal were processed simultaneously as a cohort to control for any possible differences in the solutions or antibody concentrations.

Immunoreactivity was visualized using a diaminobenzidine (DAB)-intensified horseradish peroxidase reaction. The free-floating sections were immersed in a solution containing 10 ml PBS with 5 mg DAB-tetrachloride (Sigma). Nickel sulfide (1% in water) and cobalt chloride (1% in water) were added to all DAB solutions to intensify the stain. The solution was then extracted, and the slices were re-immersed in the same DAB solution with the addition of 33 μl of 0.30% H_2O_2 for 10 min. The slices were subjected to three successive 10 min washes in PBS and then placed in a solution of 4% paraformaldehyde in PBS overnight at 4°C. On the following day, sections were washed in ascending concentrations of glycerol (40%, 80%,

and 100%) for 15 min each and then mounted in 100% glycerol. Finally, sections were coverslipped and sealed with nail polish.

Alternate sections were stained for Nissl (cresyl violet) to facilitate visualization of the laminar organization of PR as well as surrounding landmarks. After staining, these sections were covered with cytoseal 60 (Stephens Scientifics, Kalamazoo, MI, USA) and coverslipped.

Procedures for calbindin and GABA double labeling—Brains were incubated overnight at 4°C in 0.3% glutaraldehyde / 4% paraformaldehyde in PBS (also used during perfusion) followed by three 10 min washes in PBS. Inclusion of glutaraldehyde with the 4% paraformaldehyde during fixation improves GABA-immunoreactivity (Hopwood, 1967; Orkand and Kravitz, 1971) and has also been shown to improve CB-immunoreactivity in amygdalar neurons (McDonald, 1997). Horizontal sections (75 μm) were cut using a vibratome. Free-floating slices containing PR were incubated in 1% $NaBH_4$ (15 min); PBS (2X, 10 min each); 10% NGS (30 min). Slices were then incubated overnight in a solution of 3% NGS / 0.2% Triton X-100 / PBS with both anti-calbindin (mouse, Sigma) and anti-gamma-aminobutyric acid (anti-GABA; rabbit, affinity isolated, A2052, Sigma) primary antibodies each diluted 1:1000. Slices were then washed in PBS (2X, 10 min each) and incubated for 2 hr (in the dark) in 10 μg/ml of fluorescent secondary antibodies (calbindin: Alexa® Fluor® 488 goat anti-mouse IgG; GABA: Alexa® Fluor® 594 goat anti-rabbit IgG; Molecular Probes, Eugene, OR, USA). Slices were rinsed in PBS (2X, 5 min each) and mounted onto glass slides using ProLong® Antifade (Molecular Probes) mounting medium and coverslipped. Sections were stored in the freezer until used.

Antibody specificity—The anti-CB antibody was derived from a clone of the CB-955 amino acid sequence and recognizes CB in human, bovine, goat, sheep, porcine, rabbit, dog, cat, guinea-pig, rat and mouse. Technical information provided by Sigma remarks that this antibody recognized CB (28 kDa) in immunoblots and did not react with other calcium-binding proteins, including calbindin-D-9k. The anti-PV antibody was derived from a clone of the PV-19 amino acid sequence and recognizes PV in human, bovine, goat, pig, rabbit, dog, feline, rat, frog, and fish. Technical information provided by Sigma remarks that this antibody recognized PV only and did not react with other calcium-binding proteins. This antibody was also shown in muscle and brain tissue to only react with the PV (12 kDa) in immunoprecipitation (Celio and Heizmann, 1981). The anti-CR antibody was derived from recombinant rat calretinin and recognizes CR in human and rat. This antibody was shown in ferret brain tissue to only react with CR (31 kDa) in immunoblotting (Fuentes-Santamaria et al., 2005).

2.3 Quantification of immunoreactive neurons

Quantification of CB, PV, and CR immunoreactivity—A total of 51 rats from each of the three age groups were used for quantitative analyses (8 rats per group for CB; 6 rats per group for PV; 3 rats per group for CR). Alternate sections were used for analysis. Thus, six sections (50 μm) containing PR were analyzed for each animal. Every CB-, PV-, and CR-ir neuron within PR (as defined above) was counted by an individual blind to the age of the animals. Cells were counted within each of the layers of PR (I, II/III, V, and VI) for each hemisphere using a Zeiss Axioskop and a 10X air objective. Data from each section were combined (by layer and by total count) to obtain an estimate of the total number of immunoreactive cells in PR for each rat. Individual neurons were reconstructed using a drawing tube attached to a Zeiss Axioskop (using a 40X air objective).

For presentation, slices were photographed with 2.5X and 10X air objectives on a Zeiss Axioskop equipped with an Axiophot module for photography. Individual CB-, PV-, or CR-ir neurons were also photographed using 40X air objectives. Negatives were digitized professionally at 1536 × 1024 dpi and stored on CD-ROM (Imag'In Cafe' & Studio, New Haven, CT). Digital images were converted to 256-level grayscale, reduced to 80% of original size, and converted to TIFF format using GraphicConverter (Lemke Software GmbH, Peine, Germany).

Quantification of CB and GABA double-labeled tissue—An Olympus FluoView™ 300 system, equipped with argon (488 nm) and HeNe lasers (543 and 633 nm), was used for dual-fluorescence confocal microscopy. The 488 and 543 nm lines were used to image CB- and GABA-ir neurons in sequential scan mode to minimize bleed-through between the two channels. In two sections of PR from each of 6 rats (2 rats per age group), labeled neurons were classified into one of three groups: CB-ir but not GABA-ir; GABA-ir but not CB-ir; or both CB-ir and GABA-ir. The sections corresponded to brain atlas plates 98 and 99 (Paxinos and Watson, 1998). For these dual-labeling studies, a more limited portion of PR was quantified (corresponding to − 4.0 to − 4.8 mm rostro-caudal relative to Bregma).

2.4 Statistical analysis

An analysis of variance (ANOVA) was used to determine the significance of aging-related changes in the estimated number of neurons that were immunoreactive to the CaBP antibodies. A two-way ANOVA evaluated interactions between age group and cortical layer. Unless otherwise noted, if the ANOVA was significant ($\alpha = .05$), a Bonferroni-Dunn test was used for *post-hoc* comparisons. Data are reported as the mean ± 1 standard error. For the dual labeling studies, the effect size (f) was calculated for the main effect of age. Effect sizes were computed using equation 8.2.2 of Cohen (see page 275 of Cohen, 1988). The f statistic was then converted to the more widely used value (η^2) using the equation $\eta^2 = f^2 / (1 + f^2)$ (see page 281 of Cohen, 1988). Related power calculations used table 8.3.13 of Cohen (see page 313 of Cohen, 1988). In cases where the ANOVA was significant, power was based on an alpha of 0.05 and the calculated effect size. For experiments where the ANOVA was not significant, power was based on an alpha of 0.05 and a medium effect size ($f = 0.25$) was assumed.

3. Results

3.1 Laminar distribution of three calcium binding proteins in adult perirhinal cortex

As described below, an analysis of the relative frequency of immunoreactive neurons revealed distinct differences in the laminar distribution of these three CaBPs in adult PR.

CaBPs in PR layer I—Layer I was virtually devoid of CaBPs (Fig. 2). This was not surprising since layer I of PR is cell-sparse (Burwell, 2001;Furtak et al., 2007b). When averaged across rats, the mean percentage of CB-ir or PV-ir neurons in layer I was extremely low relative to the percentage of CR-ir neurons. Analysis of the mean relative frequency of each CaBP indicated a statistically significant difference in layer I ($F_{2,14} = 16.3$, $p < 0.001$). Post-hoc comparisons revealed that the mean percentage of CR-ir (2.0 ± 0.6%) in layer I of adult PR was significantly greater than the percentage of either CB-ir (0.2 ± 0.1%; $p < 0.001$) or PV-ir (0.6 ± 0.1%; $p < 0.005$). Compared with CB- or PV-immunoreactivity, the greater relative frequency of CR-ir neurons in layer I was one distinguishing feature of CR-immunoreactivity in PR (Table 1).

CaBPs in PR layer II/III—In contrast to layer I, a substantial number of neurons were immunoreactive for each of the different CaBPs in layer II/III of adult PR (see Figs. 2A-C,

Table 1). Analysis of the mean relative frequency of each CaBP indicated a statistically significant difference in layer II/III ($F_{2,14} = 89.3$, $p < 0.001$). Post-hoc comparisons revealed that the mean percentage of CB-ir (64 ± 3%) neurons in layer II/III of adult PR was significantly greater than the percentage of either PV-ir (26 ± 1%; $p < 0.001$) or CR-ir (34 ± 1%; $p < 0.001$) neurons. Thus, a distinguishing feature of CB-immunoreactivity in adult PR was the greater relative frequency of CB-ir neurons in layer II/III (Figs. 2A-C and Table 1).

CaBPs in PR layer V—Analysis of CaBP immunoreactivity in layer V of adult PR revealed a statistically significant difference in the relative frequency of the three CaBPs ($F_{2,14} = 87.1$, $p < 0.001$). The percentage of PV-ir (61 ± 1%) and CR-ir (52 ± 1%) neurons was significantly greater than the percentage of CB-ir (29 ± 2%; $p < 0.001$) neurons. One distinguishing feature of the laminar distribution of PV- and CR-immunoreactivity was the greater relative frequency of staining in layer V of adult PR (see Fig. 2 and Table 1).

CaBPs in PR layer VI—Analysis of CaBP immunoreactivity in layer VI of adult PR also revealed a statistically significant difference in the relative frequency of the three CaBPs ($F_{2,14} = 13.6$, $p < 0.001$). Post-hoc analysis revealed that the mean percentage of CB-ir (8 ± 1 %) neurons in layer VI of adult PR was significantly lower than the percentage of PV-ir (13 ± 1%; $p < 0.001$) and CR-ir (12 ± 2%; $p < 0.005$) neurons.

Laminar distribution of each CaBP in adult PR—Figure 2A illustrates the laminar distribution of CB-ir neurons throughout adult PR. One-way ANOVAs revealed a statistically significant difference in both the number ($F_{3,28} = 25.3$, $p < 0.001$) and relative frequency ($F_{3,28} = 274.7$, $p < 0.001$) of CB-ir neurons as a function of layer. The most distinguishing feature of the laminar profile of CB-immunoreactivity in adult PR was the greater number (2216 ± 388) and percentage (64 ± 3%) of CB-ir neurons in layer II/III relative to the other layers (see Fig. 2A and Table 1). Figure 2B illustrates the distribution of PV-ir neurons throughout adult PR. A statistically significant difference in both the number ($F_{3,20} = 137.1$, $p < 0.001$) and relative frequency ($F_{3,20} = 1123.7$, $p < 0.001$) of PV-ir neurons was observed as a function of layer. In contrast to CB, the most distinguishing feature of the laminar profile of PV-immunoreactivity was the greater number (983 ± 66) and percentage (61 ± 1%) of PV-ir neurons in layer V relative to the other layers (see Fig. 2B and Table 1). Evaluation of CR-ir staining in adult PR also revealed a statistically significant difference in both number ($F_{3,8} = 10.9$, $p < 0.005$) and relative frequency ($F_{3,8} = 244.2$, $p < 0.001$) of CR-ir neurons as a function of layer. Similar to PV, the most distinguishing feature of the laminar profile of CR-immunoreactivity was the greater number (1033 ± 225) and percentage (52 ± 1%) of CR-ir neurons in layer V relative to the other layers (see Fig. 2C and Table 1).

3.2 Morphology of CaBP-immunoreactive neurons in adult perirhinal cortex

The majority of neurons that were immunoreactive for any of the three CaBPs were nonpyramidal in shape (see Fig. 3). Nonpyramidal CB-ir cells consisted of bipolar, bitufted, and small and large multipolar neurons (Fig. 3A). Pyramidal CB-ir cells were less common, tended to be bifurcating pyramids in layer II/III, and were weakly stained. Occasionally, a horizontal or inverted pyramidal-like cell was encountered. In addition to the CB-ir associated with the soma and proximal dendrites of individual neurons, there was also considerable staining of the neuropil in layers II/III and V.

Nonpyramidal PV-ir neurons consisted of multipolar, bipolar, neurogliaform, stellate, and fusiform cells (see Fig. 3B). Pyramidal PV-ir neurons consisted of darkly-stained inverted and horizontal pyramidal-like neurons along with some weakly-stained upright pyramidal neurons. There was also a high amount of PV-ir staining in axonal arborizations within

layers II/III and V (see Fig. 4). The axonal arborizations formed baskets around unstained somas in layers II/III and V—a unique characteristic of basket cells (see Fig. 4). The majority of CR-ir neurons also had nonpyramidal morphologies, which consisted of bipolar, multipolar, stellate-like, and fusiform cells. A few horizontal pyramidal cells in layer VI were also CR-ir. Definitive classification of cell types was hampered by restriction of intense staining to the soma and more proximal dendrites. No obvious differences were observed among the age groups.

3.3 Selective loss of calbindin-D28k-immunoreactivity during aging

The number of CB-ir neurons was evaluated in adult, middle-aged, and aged animals (8 rats per group). When data were collapsed across layers, a statistically significant effect of age group on the mean number of CB-ir neurons in PR was observed ($F_{2,21} = 4.3$, $p < 0.05$; see Fig. 5A and Table 2). Post-hoc analysis indicated that middle-aged and aged animals contained significantly fewer CB-ir neurons in PR than adult animals ($p < 0.05$, see Fig. 5A). No significant difference was observed between middle-aged and aged rats ($p = 0.5$). A two-way ANOVA showed a significant interaction between age group and layer in the number of CB-ir neurons, $F_{6,84} = 3.0$, $p < 0.05$.

Layer II/III was the greatest contributor to the aging-related decrease in the number of CB-ir neurons (see Table 2). A one-way ANOVA indicated a significant effect of age group on the number of CB-ir neurons in layers II/III ($F_{2,21} = 3.6$, $p < 0.05$) and V ($F_{2,21} = 3.7$, $p < 0.05$). Post-hoc analysis indicated that PR of aged rats contained significantly fewer CB-ir neurons than adult PR in both layer II/III ($p < 0.02$) and layer V ($p < 0.02$). There was no significant effect of age group on the number of CB-ir neurons in layers I ($F_{2,21} = 0.5$, $p = 0.6$) or VI ($F_{2,21} = 1.4$, $p = 0.3$).

The mean number of PV-ir neurons per rat was evaluated in adult, middle-aged, and aged animals (6 rats per group). There were no significant age-related differences in the mean number of PV-ir neurons ($F_{2,15} = 0.8$, $p = 0.5$; see Fig. 5B). A two-way ANOVA also found no significant interaction between age group and layer in the mean number of PV-ir neurons ($F_{6,60}$=0.4, $p = 0.8$; see Table 2). The mean number of CR-ir neurons (3 rats per group) also did not change with age ($F_{2,6} = 0.1$, $p = 0.9$; see Fig. 5C and Table 2). There was no significant interaction between age group and cortical layer in the mean number of CR-ir neurons ($F_{6,24} = 0.2$, $p = 0.9$; see Table 2). Thus, in rat PR the only aging-related change was a decrease in the number of CB-ir neurons. Figure 6 presents a summary of the laminar distribution of each CaBP in rat PR as a function of aging.

3.4 Co-localization of GABA- and calbindin-immunoreactivity during aging

Following the initial observation of an aging-related decrease in CB-immunoreactivity in rat PR (see Fig. 5A and Table 2), we sought to determine whether these changes were due to changes in GABAergic CB-ir neurons. Simultaneous fluorescence labeling of CB and GABA indicated that most CB-ir neurons were not GABA-ir. In adult PR, only 23% of the CB-ir neurons were also immunoreactive for GABA (see Table 3). Figure 7 shows a horizontal section through PR that contains fluorescently labeled neurons that were immunoreactive for CB and/or GABA. All three possible outcomes were observed: neurons that were CB-ir but not GABA-ir (arrowhead in Fig. 7A); neurons that were GABA-ir but not CB-ir (arrow in Fig. 7B); and neurons that were both CB-ir and GABA-ir (asterisks in Figs. 6A-B). In Table 3, these three outcomes are designated “CB-ir”, “GABA-ir”, and “CB-ir and GABA-ir”.

Consistent with our previous observation (see Table 2 and Fig. 5A), there was a significant effect of age group on the mean number of neurons that were CB-ir but not GABA-ir ($F_{2,3} =$

10.4, $p < 0.05$; "CB-ir" in Table 3). The effect size for this difference was large, f = 1.11 ($\eta^2 = 0.55$), and the power was low (0.18). Post-hoc analysis indicated that aged animals had significantly fewer "CB-ir" neurons compared with the adult group ($p < 0.05$, one-tailed t-test). The middle-aged group was not statistically different from the adult group ($p = 0.06$), and there was no significant difference between the middle-aged and the aged animals ($p = 0.2$). In addition, there was no significant effect of age group on the mean number of GABA-ir neurons that did not stain for CB ("GABA-ir"; $F_{2,3} = 0.2$, $p = 0.8$, power = 0.07) or the mean number of double-labeled cells ("CB-ir and GABA-ir"; $F_{2,3} = 0.3$, $p = 0.7$, power = 0.07). When data were combined for both groups of CB-ir neurons ("CB-ir" and "CB-ir and GABA-ir" neurons), the age-related decrease was not statistically significant ($F_{2,3} = 7.6$, $p = 0.07$, power = 0.07). Thus the group of CB-ir neurons that changed across age groups was not GABAergic. This group consisted of pyramidal and nonpyramidal neurons located in layers II/III through VI of PR.

4. Discussion

The present study examined the laminar distribution of three CaBPs as a function of aging in the rodent perirhinal cortex (see Table 2). Regardless of age, there were characteristic differences in the laminar distribution of neurons that were immunoreactive for CB, PV, or CR (see Fig. 2). Aging was accompanied by a decrease in the mean number of CB-ir neurons (Fig. 5A). By contrast, no changes were detected in the number of PV- (Fig. 5B) or CR-ir neurons (Fig. 5C). Furthermore, no differences were observed in either the number of GABA-ir neurons or the number of neurons that were dual labeled for GABA and CB, suggesting that the population of CB-ir neurons that decreased during aging was not GABAergic.

4.1 Laminar distribution and morphology of CaBPs in adult rats

There were significant differences in the laminar distributions of the three CaBPs in PR, as summarized in Figure 2. Whereas PV- and CR-ir neurons were most numerous in layer V of perirhinal cortex (PR), CB-ir neurons were most numerous in layer II/III (Fig. 2 and Table 2). In non-human primates, the vast majority of the CB-ir neurons are also found in PR layers II and III (Suzuki and Porteros, 2002), suggesting that the relative distribution of calbindin in adult PR is conserved between rodents and primates. In layer I of PR, the relative frequency of CR-ir neurons was greater than the relative frequency of either CB- or PV-ir neurons (see Fig. 2D and Table 2). The functional significance of the spatial distributions of these CaBPs is currently unknown.

Based on somatic and proximal dendrite immunoreactivity, there were no morphological differences among neurons that were immunoreactive for the three different CaBPs. On the other hand, there was a unique pattern of axonal staining in brains reacted for PV, indicating that different morphological cell types may have different CaBP profiles or that the location of CaBPs may differ. Specifically, a punctate pattern of axonal PV-immunoreactivity was observed around unstained cell bodies in layers II/III and V (see Fig. 4). This pattern of axonal arborization is unique to basket cells, which are known to be GABAergic and are presumed to have an inhibitory affect on the pyramidal cells that they encase (Jones and Hendry, 1984). Similar axonal PV-ir has been reported in adjacent brain regions in the rat, such as the basolateral nuclear complex of the amygdala (McDonald and Betette, 2001) and the entorhinal cortex (Wouterlood et al., 1995).

4.2 Aging-related changes in specific CaBPs

The results show that the estimated total number of CB-ir neurons in PR decreased by approximately 50% between the adult and aged animals (Fig. 5A). This result was replicated

in a second experiment using fluorescent labeling. A decrease was found in the number of cells reactive only for CB in aged animals compared to adult animals. No significant age-related decrease was observed in the number of neurons that were dual labeled for CB and GABA (see Fig. 7 and Table 3). Previous research indicates that CB is less strictly co-localized with GABA and is more often associated with pyramidal neurons than either PV or CR (for review see DeFelipe, 1997). In the present study, only 23% of the CB-ir neurons were also immunoreactive for GABA (Fig. 7 and Table 3). This suggests that the majority of CB-ir neurons in PR may be excitatory.

The aging-related decline in the number of CB-ir neurons is subject to at least two different interpretations. On the one hand, the decline could reflect preferential cell death in these neurons in PR during normal aging. However, recent data suggest that neuron number does not significantly decrease in rat PR during aging, even in cognitively impaired animals (Rapp et al., 2002). A more likely interpretation is that the observed aging-related decrease in CB-immunoreactivity reflects a selective loss of intracellular calbindin production (either in gene transcription or mRNA translation), reflective of a general shift in the mRNA expression profile in PR during aging. Indeed, several studies have demonstrated that aging results in a down regulation of CB mRNA in several brain regions, including hippocampus (Iacopino and Christakos, 1990; Kishimoto et al., 1998).

Decreased CB expression in PR neurons could contribute to dysregulation of the intracellular calcium ion concentration (particularly during prolonged periods of high activity) and thereby render PR neurons more susceptible to dysfunction, excitotoxicity, and cell death (Iacopino and Christakos, 1990). The consequences of cell death or dysfunction may not only depend upon the normal neurophysiological role of this specific class of PR neuron (i.e., the CB-ir neuron that is *not* GABAergic) but also on any compensatory changes that may occur (e.g., upregulation of other endogenous CaBPs). The results encourage further neurobiological research into mechanisms of aging-related changes in CaBP expression.

In contrast to CB-ir neurons, the number of PV- and CR-ir neurons remained stable during normal aging in rat PR (Table 2; Figs. 5B,C). These data are consistent with previous studies, which also demonstrated preserved numbers of PV- or CR-ir neurons in hippocampus during normal aging (de Jong et al., 1996;Kishimoto et al., 1998;Potier et al., 1994). Although CR-ir neurons did not change significantly in PR during aging, the statistical power was low (0.06), partly due to the small sample size (n = 3 per age group).

4.3 Comparisons with other animal research

There have been no other studies of the distribution of calbindin, parvalbumin, or calretinin in rat PR. However, these CaBPs have been examined in other brain structures and in other species. Studies of rat and rabbit hippocampus reported two similarities to the present results. First, the number of CB-ir neurons was found to decrease in aged animals compared to adult animals (Krzywkowski et al., 1996; Potier et al., 1994; Villa et al., 1994). Second, the number of PV- and CR-ir neurons was reported not to change in aged compared to adult animals (Krzywkowski et al., 1996; Lolova and Davidoff, 1992; Potier et al., 1994). Similarly, a study by de Jong and colleagues (1996) demonstrated that the number of PV-ir neurons did not change in aged rat or rabbit hippocampus; however, they did observe a decrease in the density of PV-ir axonal arborizations in aged hippocampus (de Jong et al., 1996). Since axonal arborizations were not quantified in the present study, it is possible that similar deceases may also occur in rat PR during aging.

One difference between the hippocampus and PR is that the aging-related decrease in CB expression in hippocampus is thought to be due to a loss of GABAergic neurons

(Krzywkowski et al., 1996) whereas the present data from PR suggest that calbindin expression is lost primarily in neurons that are not GABAergic (Table 3; see also Fig. 7). Although the number of GABA-ir neurons did not change as a function of aging (Table 3), the small sample size (n = 2 animals per age group) leaves open the possibility that a larger sample might have revealed subtle aging-related changes in the number of GABA-ir neurons in PR.

4.4 Clinical implications of calcium dysregulation

Deficits in human mnemonic function have been reported during normal aging and more substantially in various aging-related diseases, including mild cognitive impairment and AD. Understanding the underlying neurobiological modifications that produce these behavioral deficits is important for therapeutic advancements. One unifying hypothesis suggests that the disruption of cellular calcium homeostasis is intimately involved not only in the memory impairments that accompany normal aging but also in the pathologies associated with aging-related neurodegenerative disorders (Disterhoft et al., 1994; Khachaturian, 1987, 1994; Landfield, 1987).

Multiple lines of evidence implicate alterations in calcium signaling (including changes in CaBPs) during aging and aging-related neurodegenerative disorders (for review, see Mattson, 2007). For example, individuals diagnosed with AD have significantly fewer CB-ir neurons in frontal, temporal and parietal cortices (Ichimiya et al., 1988; Lally et al., 1997; Mikkonen et al., 1999). AD patients also tend to have well-preserved levels of PV- and CR-immunoreactivity in several cortical areas (Brion and Resibois, 1994; Hof et al., 1991; Solodkin et al., 1996). Recent data using transgenic mice that express human amyoid precursor proteins (hAPP) and amyloid-β peptides (Aβ) further suggest a direct link between calbindin expression, AD pathology, and cognitive decline. The transgenic mice had a significant reduction in hippocampal CB-immunoreactivity that was tightly correlated with age and the relative abundance of Aβ (Palop et al., 2003). The decreased CB expression was highly correlated with spatial memory impairments such that mice with the lowest levels of CB exhibited the most profound spatial memory deficits. Thus, in patients with AD, reductions in CB expression may actually contribute to cognitive deficits.

A significant loss of CB expression in PR during normal aging may contribute to a cellular environment that renders neurons more susceptible to dysfunction and degeneration. Because the decrease in CB was observed in PR of middle-aged animals, it is likely to be an early indication of cellular dysfunction during aging. Although similar studies in humans have not focused on PR, a study of AD patients and age-matched controls revealed a negative correlation between age and the ratio of CB-ir neurons within layer II of Brodmann's area 22 of the temporal lobe in the control subjects as well as an overall decrease in CB in the AD patients (Nishiyama et al., 1993). A link between disruption of intracellular calcium regulation and neurodegenerative disorders has been well established (for review, see Mattson, 2007), but little is known about precisely how changes in CaBP expression during normal aging influence or are affected by neurodegenerative disease progression.

CB and other CaBPs may serve an important role in neuroprotection (Mattson et al., 1991). Furthermore, the actual level of expression of CaBPs within a neuron may influence the susceptibility to various neurodegenerative disorders. For example, in the frontal cortex (Brodmann area 9) layer III pyramidal neurons that were weakly immunoreactive for CB were the most vulnerable to degeneration whereas the heavily CB-ir interneurons in layers II-III were resistant to degeneration in AD (Hof and Morrison, 1991). The reduction in CaBPs observed in transgenic mice that express APP alone or in conjunction with PS1 mutations (Palop et al., 2003; Popovic et al., 2008) suggest that AD pathology may actually

affect CaBP expression, further rendering exposed neurons susceptible to calcium overload as part of a vicious cycle of neuronal degeneration.

4.5 Conclusions

The present study is the first to report an aging-related decrease in the number of CB-ir neurons in rat PR. These changes first appeared in the middle-aged animals suggesting that altered CaBP expression may be an important early marker for future impairment in perirhinal function with advancing age. The present data, in conjunction with the observation that the distribution of PR CB-ir neurons is conserved across adult rodents and primates (Suzuki and Porteros, 2002), motivate studies of CaBP expression in PR during the primate life span. Importantly, middle-aged rats appear not to be significantly impaired in two PR-dependent tasks—trace and contextual fear conditioning (Bang and Brown, 2009; Bucci et al., 2000; Kholodar-Smith et al., 2008; Lindquist et al., 2004; Moyer and Brown, 2006). The fact that there is a detectable decrease in CB-ir in PR in middle-aged animals, prior to the onset of widespread cognitive deficits that typically accompany aging, indicates a therapeutic window for intervention that may be useful for protecting the aging brain and thwarting age-related memory deficits. Thus aging-related alterations in CaBP expression may be a novel target for minimizing neurodegeneration during aging in humans. The present findings suggest that animal models may offer useful experimental advantages for exploring the nature of the relationship between aging, alterations in CaBP expression, and learning and memory.

Acknowledgments

This work was supported by NIH grants RO1 AG19645 and RO1 MH58405 to THB. The authors thank N. Kelsey, B. Payne, and L. Wygant for technical assistance.

REFERENCES

Amenta F, Cavalotta D, Del Valle ME, Mancini M, Sabbatini M, Torres JM, Vega JA. Calbindin D-28k immunoreactivity in the rat cerebellar cortex: age-related changes. Neurosci Lett. 1994; 178:131–134. [PubMed: 7816322]

Andressen C, Blumcke I, Celio MR. Calcium-binding proteins: selective markers of nerve cells. Cell Tissue Res. 1993; 271:181–208. [PubMed: 8453652]

Babcock DF, Herrington J, Goodwin PC, Park YB, Hille B. Mitochondrial participation in the intracellular Ca2+ network. J Cell Biol. 1997; 136:833–844. [PubMed: 9049249]

Baimbridge KG, Celio MR, Rogers JH. Calcium-binding proteins in the nervous system. Trends Neurosci. 1992; 15:303–308. [PubMed: 1384200]

Bang SJ, Brown TH. Perirhinal cortex supports acquired fear of auditory objects. Neurobiol Learn Mem. 2009; 92:53–62. [PubMed: 19185613]

Barker GR, Bird F, Alexander V, Warburton EC. Recognition memory for objects, place, and temporal order: a disconnection analysis of the role of the medial prefrontal cortex and perirhinal cortex. J Neurosci. 2007; 27:2948–2957. [PubMed: 17360918]

Braak H, Braak E. Morphological criteria for the recognition of Alzheimer's disease and the distribution pattern of cortical changes related to this disorder. Neurobiol Aging. 1994; 15:355–356. discussion 379–380. [PubMed: 7936061]

Braak H, Braak E. Staging of Alzheimer's disease-related neurofibrillary changes. Neurobiol Aging. 1995; 16:271–278. discussion 278–284. [PubMed: 7566337]

Brion JP, Resibois A. A subset of calretinin-positive neurons are abnormal in Alzheimer's disease. Acta Neuropathol (Berl). 1994; 88:33–43. [PubMed: 7941970]

Brown, TH.; Byrne, JH.; Lebar, K.; LeDoux, J.; Lindquist, DH.; Thompson, RF.; Teyler, TJ. Learning and memory: Basic mechanisms. In: Byrne, JH.; Roberts, JL., editors. Cellular and molecular neuroscience. Academic Press; San Diego: 2004. p. 499-583.

Brown, TH.; Zhao, Y.; Leung, V. Hebbian Synapses. In: Squire, LR., editor. Encyclopedia of Neuroscience. Academic Press; Oxford: 2008.

Bu J, Sathyendra V, Nagykery N, Geula C. Age-related changes in calbindin-D28k, calretinin, and parvalbumin-immunoreactive neurons in the human cerebral cortex. Exp Neurol. 2003; 182:220–231. [PubMed: 12821392]

Bucci DJ, Phillips RG, Burwell RD. Contributions of postrhinal and perirhinal cortex to contextual information processing. Behav Neurosci. 2000; 114:882–894. [PubMed: 11085602]

Buckley MJ, Gaffan D. Learning and transfer of object-reward associations and the role of the perirhinal cortex. Behav Neurosci. 1998a; 112:15–23. [PubMed: 9517812]

Buckley MJ, Gaffan D. Perirhinal cortex ablation impairs configural learning and paired-associate learning equally. Neuropsychologia. 1998b; 36:535–546. [PubMed: 9705064]

Buffalo EA, Bellgowan PS, Martin A. Distinct roles for medial temporal lobe structures in memory for objects and their locations. Learn Mem. 2006; 13:638–643. [PubMed: 16980544]

Burwell RD. Borders and cytoarchitecture of the perirhinal and postrhinal cortices in the rat. J Comp Neurol. 2001; 437:17–41. [PubMed: 11477594]

Burwell RD, Amaral DG. Perirhinal and postrhinal cortices of the rat: interconnectivity and connections with the entorhinal cortex. J Comp Neurol. 1998; 391:293–321. [PubMed: 9492202]

Burwell RD, Witter MP, Amaral DG. Perirhinal and postrhinal cortices of the rat: a review of the neuroanatomical literature and comparison with findings from the monkey brain. Hippocampus. 1995; 5:390–408. [PubMed: 8773253]

Bussey TJ, Saksida LM, Murray EA. Perirhinal cortex resolves feature ambiguity in complex visual discriminations. Eur J Neurosci. 2002; 15:365–374. [PubMed: 11849302]

Campbell LW, Hao SY, Thibault O, Blalock EM, Landfield PW. Aging changes in voltage-gated calcium currents in hippocampal CA1 neurons. J Neurosci. 1996; 16:6286–6295. [PubMed: 8815908]

Celio MR, Heizmann CW. Calcium-binding protein parvalbumin as a neuronal marker. Nature. 1981; 293:300–302. [PubMed: 7278987]

Choi DW. Excitotoxic cell death. J Neurobiol. 1992; 23:1261–1276. [PubMed: 1361523]

Choi DW. Calcium and excitotoxic neuronal injury. Ann N Y Acad Sci. 1994; 747:162–171. [PubMed: 7847669]

Cohen, J. Statistical Power Analysis for the Behavioral Sciences. Lawrence Erlbaum Associates; Hillsdale, NJ: 1988.

de Jong GI, Naber PA, Van der Zee EA, Thompson LT, Disterhoft JF, Luiten PG. Age-related loss of calcium binding proteins in rabbit hippocampus. Neurobiol Aging. 1996; 17:459–465. [PubMed: 8725908]

DeFelipe J. Types of neurons, synaptic connections and chemical charactersitics of cells immunoreactive for calbindin-D28k, parvalbumin and calretinin in the neorcortex. J Chem Neuroanat. 1997; 14:1–19. [PubMed: 9498163]

Detoledo-Morrell L, Sullivan MP, Morrell F, Wilson RS, Bennett DA, Spencer S. Alzheimer's disease: in vivo detection of differential vulnerability of brain regions. Neurobiol Aging. 1997; 18:463–468. [PubMed: 9390771]

Deyo RA, Straube KT, Disterhoft JF. Nimodipine facilitates associative learning in aging rabbits. Science. 1989; 243:809–811. [PubMed: 2916127]

Dickerson BC, Feczko E, Augustinack JC, Pacheco J, Morris JC, Fischl B, Buckner RL. Differential effects of aging and Alzheimer's disease on medial temporal lobe cortical thickness and surface area. Neurobiol Aging. 2009; 30:432–440. [PubMed: 17869384]

Disterhoft JF, Moyer JR Jr. Thompson LT. The calcium rationale in aging and Alzheimer's disease. Evidence from an animal model of normal aging. Ann N Y Acad Sci. 1994; 747:382–406. [PubMed: 7847686]

Disterhoft JF, Moyer JR Jr. Thompson LT, Kowalska M. Functional aspects of calcium-channel modulation. Clin Neuropharmacol. 1993; 16(Suppl 1):S12–24. [PubMed: 8390916]

Eacott MJ, Norman G. Integrated memory for object, place, and context in rats: a possible model of episodic-like memory? J Neurosci. 2004; 24:1948–1953. [PubMed: 14985436]

Eichenbaum H, Yonelinas AP, Ranganath C. The medial temporal lobe and recognition memory. Annu Rev Neurosci. 2007; 30:123–152. [PubMed: 17417939]

Foster TC. Calcium homeostasis and modulation of synaptic plasticity in the aged brain. Aging Cell. 2007; 6:319–325. [PubMed: 17517041]

Fuentes-Santamaria V, Alvarado JC, Taylor AR, Brunso-Bechtold JK, Henkel CK. Quantitative changes in calretinin immunostaining in the cochlear nuclei after unilateral cochlear removal in young ferrets. J Comp Neurol. 2005; 483:458–475. [PubMed: 15700274]

Furtak SC, Allen TA, Brown TH. Single-unit firing in rat perirhinal cortex caused by fear conditioning to arbitrary and ecological stimuli. J Neurosci. 2007a; 27:12277–12291. [PubMed: 17989293]

Furtak SC, Moyer JR Jr. Brown TH. Morphology and ontogeny of rat perirhinal cortical neurons. J Comp Neurol. 2007b; 505:493–510. [PubMed: 17924570]

Furtak SC, Wei SM, Agster KL, Burwell RD. Functional neuroanatomy of the parahippocampal region in the rat: the perirhinal and postrhinal cortices. Hippocampus. 2007c; 17:709–722. [PubMed: 17604355]

Hannesson DK, Howland JG, Phillips AG. Interaction between perirhinal and medial prefrontal cortex is required for temporal order but not recognition memory for objects in rats. J Neurosci. 2004; 24:4596–4604. [PubMed: 15140931]

Heizmann CW. Calcium-binding proteins of the EF-type. J Cardiovasc Pharmacol. 1988; 12(Suppl 5):S30–37. [PubMed: 2469875]

Hof PR, Cox K, Young WG, Celio MR, Rogers J, Morrison JH. Parvalbumin-immunoreactive neurons in the neocortex are resistant to degeneration in Alzheimer's disease. J Neuropathol Exp Neurol. 1991; 50:451–462. [PubMed: 2061713]

Hof PR, Morrison JH. Neocortical neuronal subpopulations labeled by a monoclonal antibody to calbindin exhibit differential vulnerability in Alzheimer's disease. Exp Neurol. 1991; 111:293–301. [PubMed: 1999232]

Holdstock JS, Gutnikov SA, Gaffan D, Mayes AR. Perceptual and mnemonic matching-to-sample in humans: contributions of the hippocampus, perirhinal and other medial temporal lobe cortices. Cortex. 2000; 36:301–322. [PubMed: 10921661]

Hopwood D. Some aspects of fixation with glutaraldehyde. A biochemical and histochemical comparison of the effects of formaldehyde and glutaraldehyde fixation on various enzymes and glycogen, with a note on penetration of glutaraldehyde into liver. J Anat. 1967; 101:83–92. [PubMed: 6047703]

Iacopino AM, Christakos S. Specific reduction of calcium-binding protein (28-kilodalton calbindin-D) gene expression in aging and neurodegenerative diseases. Proc Natl Acad Sci U S A. 1990; 87:4078–4082. [PubMed: 2140897]

Ichimiya Y, Emson PC, Mountjoy CQ, Lawson DE, Heizmann CW. Loss of calbindin-28K immunoreactive neurones from the cortex in Alzheimer-type dementia. Brain Res. 1988; 475:156–159. [PubMed: 3214722]

Jones, EG.; Hendry, SH. Basket cells. In: Peters, A.; Jones, EG., editors. Cerebral Cortex: Cellular Components of the Cerebral Cortex. Vol. 1. Plenum Press; New York: 1984. p. 309-336.

Juottonen K, Laakso MP, Insausti R, Lehtovirta M, Pitkanen A, Partanen K, Soininen H. Volumes of the entorhinal and perirhinal cortices in Alzheimer's disease. Neurobiol Aging. 1998; 19:15–22. [PubMed: 9562498]

Khachaturian ZS. Hypothesis on the regulation of cytosol calcium concentration and the aging brain. Neurobiol Aging. 1987; 8:345–346. [PubMed: 3627349]

Khachaturian ZS. Calcium hypothesis of Alzheimer's disease and brain aging. Ann N Y Acad Sci. 1994; 747:1–11. [PubMed: 7847664]

Kholodar-Smith DB, Boguszewski P, Brown TH. Auditory trace fear conditioning requires perirhinal cortex. Neurobiol Learn Mem. 2008; 90:537–543. [PubMed: 18678265]

Kishimoto J, Tsuchiya T, Cox H, Emson PC, Nakayama Y. Age-related changes of calbindin-D28k, calretinin, and parvalbumin mRNAs in the hamster brain. Neurobiol Aging. 1998; 19:77–82. [PubMed: 9562507]

Kruman, Mattson MP. Pivotal role of mitochondrial calcium uptake in neural cell apoptosis and necrosis. J Neurochem. 1999; 72:529–540. [PubMed: 9930724]

Krzywkowski P, Potier B, Billard JM, Dutar P, Lamour Y. Synaptic mechanisms and calcium binding proteins in the aged rat brain. Life Sci. 1996; 59:421–428. [PubMed: 8761330]

LaFrance R, Brustovetsky N, Sherburne C, Delong D, Dubinsky JM. Age-related changes in regional brain mitochondria from Fischer 344 rats. Aging Cell. 2005; 4:139–145. [PubMed: 15924570]

Lally G, Faull RL, Waldvogel HJ, Ferrari S, Emson PC. Calcium homeostasis in ageing: studies on the calcium binding protein calbindin D28K. J Neural Transm. 1997; 104:1107–1112. [PubMed: 9503262]

Landfield PW. 'Increased calcium-current' hypothesis of brain aging. Neurobiol Aging. 1987; 8:346–347. [PubMed: 3627350]

Leslie SW, Chandler LJ, Barr EM, Farrar RP. Reduced calcium uptake by rat brain mitochondria and synaptosomes in response to aging. Brain Res. 1985; 329:177–183. [PubMed: 3978439]

Lindquist DH, Jarrard LE, Brown TH. Perirhinal cortex supports delay fear conditioning to rat ultrasonic social signals. J Neurosci. 2004; 24:3610–3617. [PubMed: 15071109]

Liu P, Bilkey DK. Excitotoxic lesions centered on perirhinal cortex produce delay-dependent deficits in a test of spatial memory. Behav Neurosci. 1998; 112:512–524. [PubMed: 9676969]

Lolova I, Davidoff M. Age-related morphological and morphometrical changes in parvalbumin- and calbindin-immunoreactive neurons in the rat hippocampal formation. Mech Ageing Dev. 1992; 66:195–211. [PubMed: 1365845]

Mattson MP. Calcium and neurodegeneration. Aging Cell. 2007; 6:337–350. [PubMed: 17328689]

Mattson MP, Rychlik B, Chu C, Christakos S. Evidence for calcium-reducing and excito-protective roles for the calcium-binding protein calbindin-D28k in cultured hippocampal neurons. Neuron. 1991; 6:41–51. [PubMed: 1670921]

McDonald AJ. Calbindin-D28k immunoreactivity in the rat amygdala. J Comp Neurol. 1997; 383:231–244. [PubMed: 9182851]

McDonald AJ, Betette RL. Parvalbumin-containing neurons in the rat basolateral amygdala: morphology and co-localization of Calbindin-D(28k). Neuroscience. 2001; 102:413–425. [PubMed: 11166127]

Meunier M, Bachevalier J, Mishkin M, Murray EA. Effects on visual recognition of combined and separate ablations of the entorhinal and perirhinal cortex in rhesus monkeys. J Neurosci. 1993; 13:5418–5432. [PubMed: 8254384]

Mikkonen M, Alafuzoff I, Tapiola T, Soininen H, Miettinen R. Subfield- and layer-specific changes in parvalbumin, calretinin and calbindin-D28K immunoreactivity in the entorhinal cortex in Alzheimer's disease. Neuroscience. 1999; 92:515–532. [PubMed: 10408601]

Mikkonen M, Soininen H, Pitkanen A. Distribution of parvalbumin-, calretinin-, and calbindin-D28k-immunoreactive neurons and fibers in the human entorhinal cortex. J Comp Neurol. 1997; 388:64–88. [PubMed: 9364239]

Molinari S, Battini R, Ferrari S, Pozzi L, Killcross AS, Robbins TW, Jouvenceau A, Billard JM, Dutar P, Lamour Y, Baker WA, Cox H, Emson PC. Deficits in memory and hippocampal long-term potentiation in mice with reduced calbindin D28K expression. Proc Natl Acad Sci U S A. 1996; 93:8028–8033. [PubMed: 8755597]

Moyer JR Jr. Brown TH. Impaired trace and contextual fear conditioning in aged rats. Behav Neurosci. 2006; 120:612–624. [PubMed: 16768613]

Moyer JR Jr. Disterhoft JF. Nimodipine decreases calcium action potentials in rabbit hippocampal CA1 neurons in an age-dependent and concentration-dependent manner. Hippocampus. 1994; 4:11–17. [PubMed: 8061749]

Moyer JR Jr. Thompson LT, Black JP, Disterhoft JF. Nimodipine increases excitability of rabbit CA1 pyramidal neurons in an age- and concentration-dependent manner. J Neurophysiol. 1992; 68:2100–2109. [PubMed: 1491260]

Murray EA, Bussey TJ, Saksida LM. Visual perception and memory: a new view of medial temporal lobe function in primates and rodents. Annu Rev Neurosci. 2007; 30:99–122. [PubMed: 17417938]

Nicholls DG. A role for the mitochondrion in the protection of cells against calcium overload? Prog Brain Res. 1985; 63:97–106. [PubMed: 3835584]

Nishiyama E, Ohwada J, Iwamoto N, Arai H. Selective loss of calbindin D28K-immunoreactive neurons in the cortical layer II in brains of Alzheimer's disease: a morphometric study. Neurosci Lett. 1993; 163:223–226. [PubMed: 8309638]

Orkand PM, Kravitz EA. Localization of the sites of gamma-aminobutyric acid (GABA) uptake in lobster nerve-muscle preparations. J Cell Biol. 1971; 49:75–89. [PubMed: 5555581]

Palop JJ, Jones B, Kekonius L, Chin J, Yu GQ, Raber J, Masliah E, Mucke L. Neuronal depletion of calcium-dependent proteins in the dentate gyrus is tightly linked to Alzheimer's disease-related cognitive deficits. Proc Natl Acad Sci U S A. 2003; 100:9572–9577. [PubMed: 12881482]

Parsana, AJ.; Brown, TH. Temporal lobe and object recognition. In: Thompson, RF.; Shors, TJ., editors. Encyclopedia of Behavioral Neuroscience. Elsevier Science; Oxford: in press

Paxinos, G.; Watson, C. The rat brain in stereotaxic coordinates. Academic Press; San Diego: 1998.

Popovic M, Caballero-Bleda M, Kadish I, Van Groen T. Subfield and layer-specific depletion in calbindin-D28K, calretinin and parvalbumin immunoreactivity in the dentate gyrus of amyloid precursor protein/presenilin 1 transgenic mice. Neuroscience. 2008; 155:182–191. [PubMed: 18583063]

Potier B, Krzywkowski P, Lamour Y, Dutar P. Loss of calbindin-immunoreactivity in CA1 hippocampal stratum radiatum and stratum lacunosum-moleculare interneurons in the aged rat. Brain Res. 1994; 661:181–188. [PubMed: 7834368]

Rapp PR, Deroche PS, Mao Y, Burwell RD. Neuron number in the parahippocampal region is preserved in aged rats with spatial learning deficits. Cereb Cortex. 2002; 12:1171–1179. [PubMed: 12379605]

Solodkin A, Veldhuizen SD, Van Hoesen GW. Contingent vulnerability of entorhinal parvalbumin-containing neurons in Alzheimer's disease. J Neurosci. 1996; 16:3311–3321. [PubMed: 8627368]

Squire LR, Wixted JT, Clark RE. Recognition memory and the medial temporal lobe: a new perspective. Nat Rev Neurosci. 2007; 8:872–883. [PubMed: 17948032]

Suzuki WA, Porteros A. Distribution of calbindin D-28k in the entorhinal, perirhinal, and parahippocampal cortices of the macaque monkey. J Comp Neurol. 2002; 451:392–412. [PubMed: 12210132]

Thibault O, Hadley R, Landfield PW. Elevated postsynaptic [Ca2+]i and L-type calcium channel activity in aged hippocampal neurons: relationship to impaired synaptic plasticity. J Neurosci. 2001; 21:9744–9756. [PubMed: 11739583]

Thibault O, Landfield PW. Increase in single L-type calcium channels in hippocampal neurons during aging. Science. 1996; 272:1017–1020. [PubMed: 8638124]

Thibault O, Porter NM, Chen KC, Blalock EM, Kaminker PG, Clodfelter GV, Brewer LD, Landfield PW. Calcium dysregulation in neuronal aging and Alzheimer's disease: history and new directions. Cell Calcium. 1998; 24:417–433. [PubMed: 10091010]

van Brederode JF, Helliesen MK, Hendrickson AE. Distribution of the calcium-binding proteins parvalbumin and calbindin-D28k in the sensorimotor cortex of the rat. Neuroscience. 1991; 44:157–171. [PubMed: 1770994]

Van Brederode JF, Mulligan KA, Hendrickson AE. Calcium-binding proteins as markers for subpopulations of GABAergic neurons in monkey striate cortex. J Comp Neurol. 1990; 298:1–22. [PubMed: 2170466]

Van Hoesen GW, Solodkin A. Cellular and system neuroanatomical changes in Alzheimer's disease. Ann N Y Acad Sci. 1994; 747:12–35. [PubMed: 7847666]

Veng LM, Mesches MH, Browning MD. Age-related working memory impairment is correlated with increases in the L-type calcium channel protein alpha1D (Cav1.3) in area CA1 of the hippocampus and both are ameliorated by chronic nimodipine treatment. Brain Res Mol Brain Res. 2003; 110:193–202. [PubMed: 12591156]

Villa A, Podini P, Panzeri MC, Racchetti G, Meldolesi J. Cytosolic Ca2+ binding proteins during rat brain ageing: loss of calbindin and calretinin in the hippocampus, with no change in the cerebellum. Eur J Neurosci. 1994; 6:1491–1499. [PubMed: 8000572]

Wouterlood FG, Hartig W, Bruckner G, Witter MP. Parvalbumin-immunoreactive neurons in the entorhinal cortex of the rat: localization, morphology, connectivity and ultrastructure. J Neurocytol. 1995; 24:135–153. [PubMed: 7745443]

Yap KL, Ames JB, Swindells MB, Ikura M. Diversity of conformational states and changes within the EF-hand protein superfamily. Proteins. 1999; 37:499–507. [PubMed: 10591109]

Zola-Morgan S, Squire LR, Clower RP, Rempel NL. Damage to the perirhinal cortex exacerbates memory impairment following lesions to the hippocampal formation. J Neurosci. 1993; 13:251–265. [PubMed: 8423472]

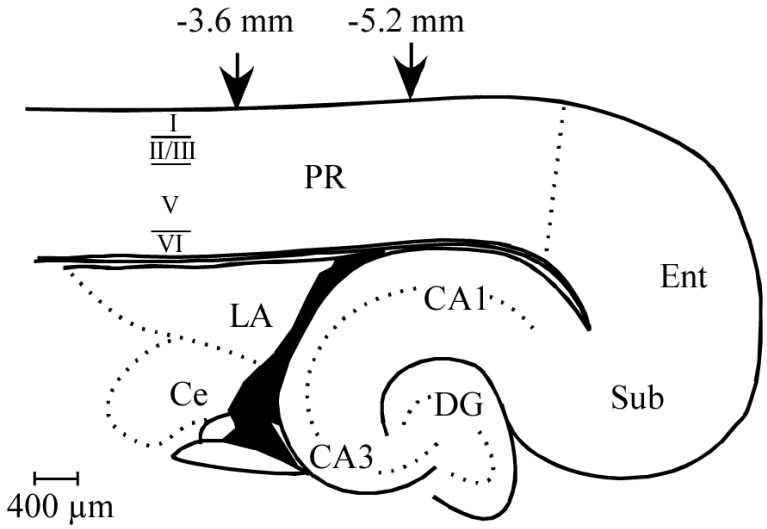

Figure 1.

Schematic diagram of rat perirhinal cortex. A horizontal brain slice containing rat perirhinal cortex (PR) with the relative laminar boarders indicated on the left side. Neuronal counting and digital analyses were conducted within the rostro-caudal boundaries of PR indicated by the downward arrows. Abbreviations: *CA1*, area CA1 of the hippocampal formation; *CA3*, area CA3 of the hippocampal formation; *Ce*, Central Nucleus of the Amygdala; *DG*, Dentate Gyrus; *LA*, lateral nucleus of the amygdala; *Ent*, entorhinal cortex; *PR*, perirhinal cortex; *Sub*, subiculum.

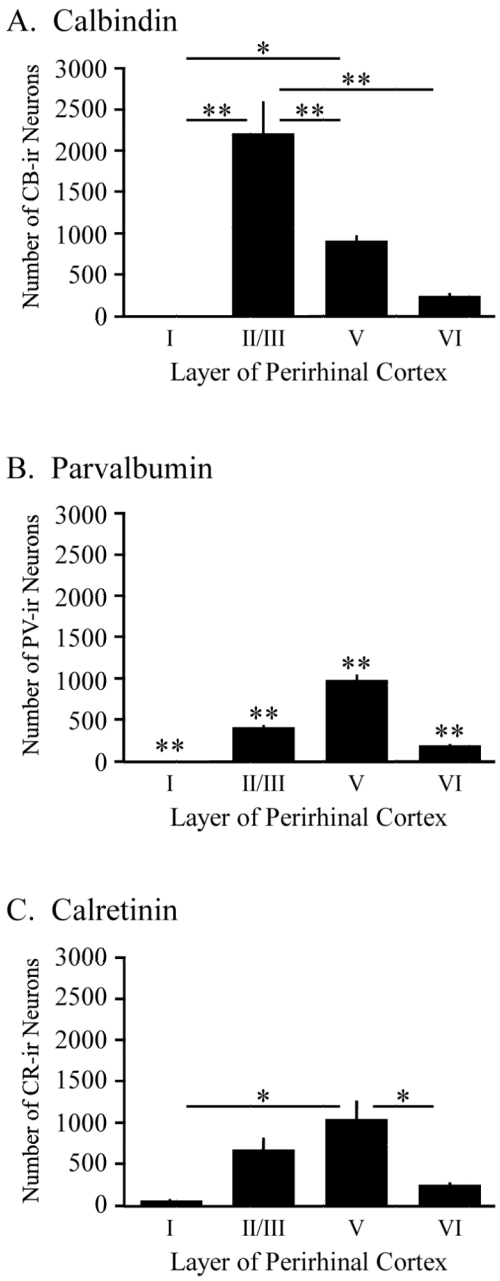

Figure 2.

Laminar distribution of three calcium binding proteins (CaBPs) in adult rat perirhinal cortex. (A-C) The number of calbindin (CB), parvabumin (PV), and calretinin (CR) immunoreactive (-ir) neurons as a function of cortical layer in adult perirhinal cortex. Notice that the greatest proportion of CB-ir neurons are found in layer II/III whereas the greatest proportion of PV- or CR-ir neurons are found in layer V. Asterisks above the horizontal lines in panels A and C indicate statistically significant differences between layers (* $p < 0.005$; ** $p < 0.001$). Asterisks above each bar in panel B indicate that each layer is statistically significantly different from the other layers (** $p < 0.001$).

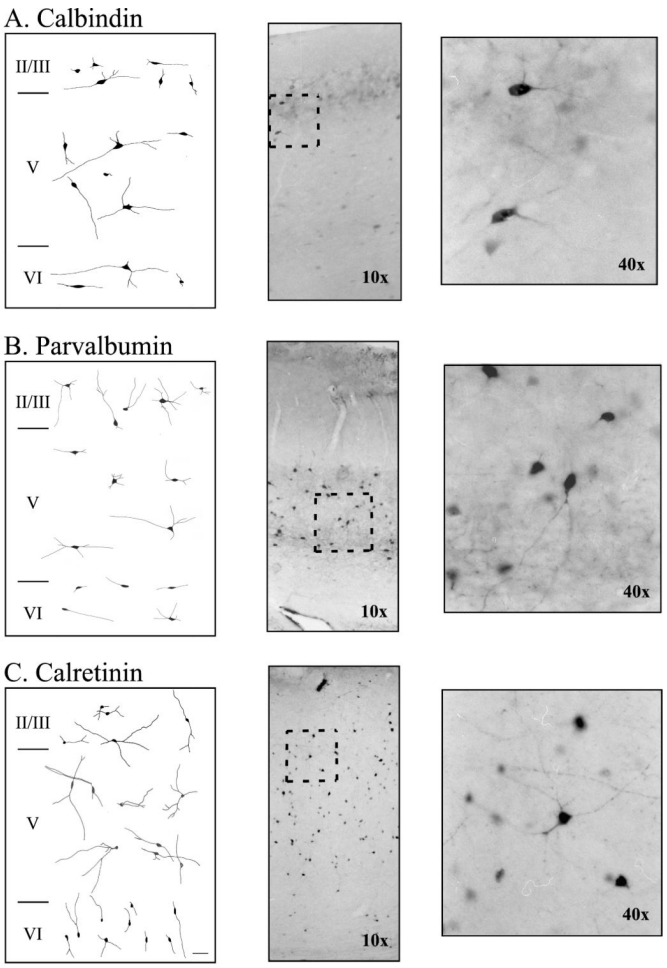

Figure 3.

Morphology of neurons immunoreactive for calcium binding proteins in adult rat perirhinal cortex. (A-C) Representative neuronal morphologies of calbindin-, parvalbumin, and calretinin-immunoreactive neurons in perirhinal layers II/III, V, and VI. The left panel shows camera lucida reconstructions, the middle panel shows a representative photograph using a 10X air objective. The area inside the rectangle is magnified (using a 40X air objective) and shown in the right panel.

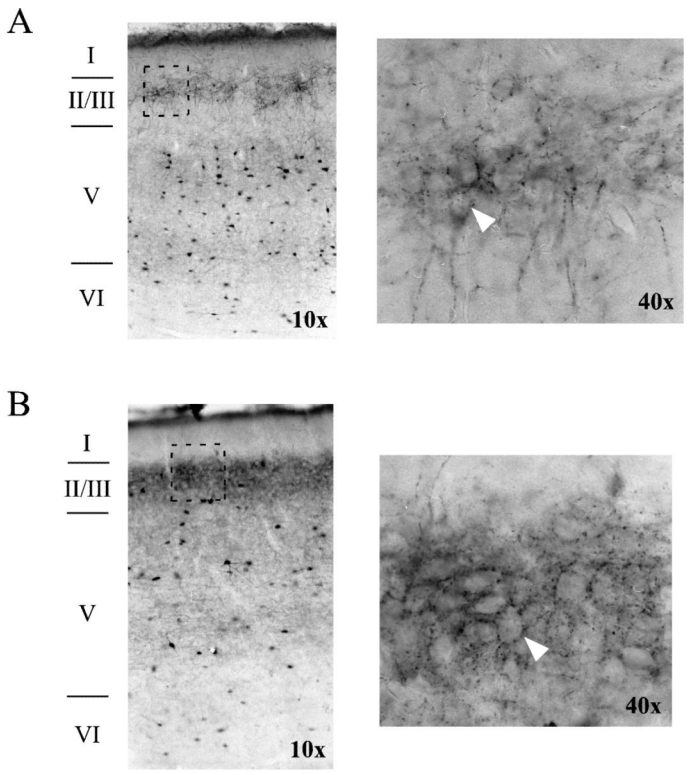

Figure 4.

Axons immunoreactive for parvalbumin form baskets around unstained cell bodies in rat perirhinal cortex. (A) Horizontal section from an adult animal taken at −7.6 mm D/V relative to Bregma. On the left is an image from a 10X air objective, showing all layers of PR. The area in the rectangle (in layer II/III) is shown on the right using a 40X air objective. The arrowhead points to the outline of a cell body. (B) Horizontal section from a middle-aged animal taken at −7.34 relative to Bregma. Images on the left and right, respectively, were taken using 10X and 40X air objectives. The arrowhead points to the outline of a cell body.

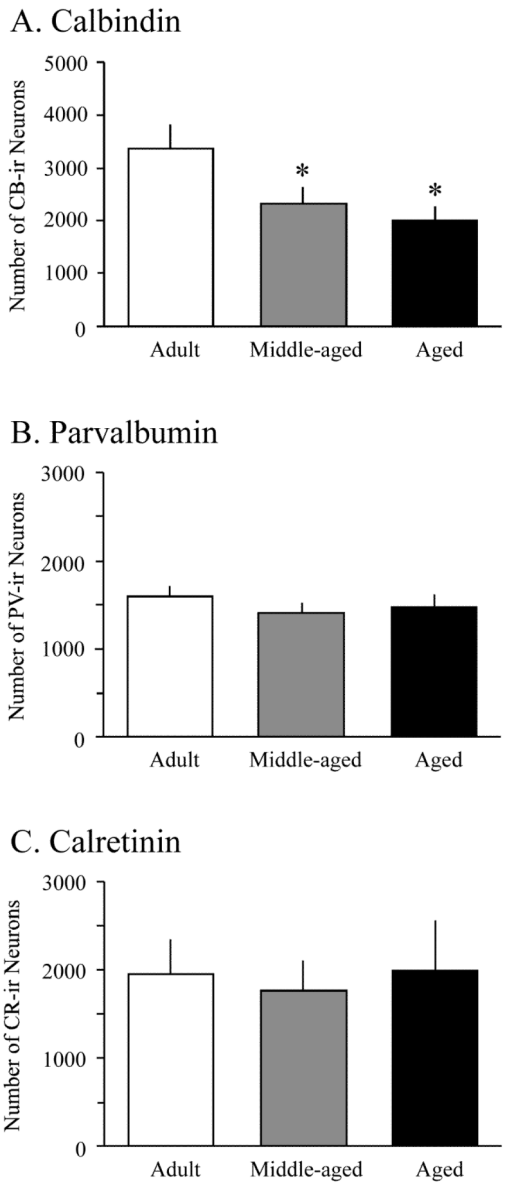

Figure 5.

Aging-related changes in CaBP expression in rat perirhinal cortex. (A) Aging results in a reduction in numbers of CB-ir neurons in rat perirhinal cortex (PR). Notice that statistically significant reductions in the number of CB-ir neurons are observed in both middle-aged and aged animals (asterisks, $p < 0.05$). (B) Stable numbers of PV-ir neurons during aging. (C) Stable numbers of CR-ir neurons during aging.

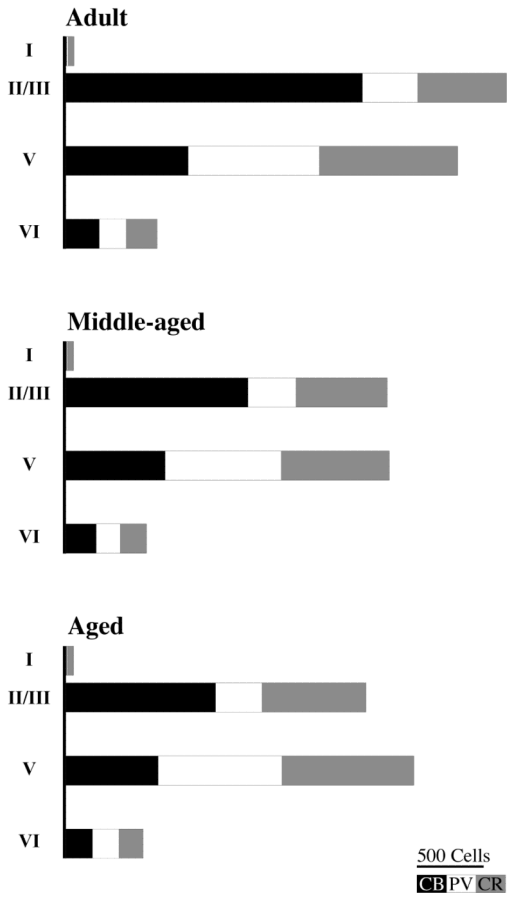

Figure 6.
Summary of calcium binding protein (CaBP) distribution in rat perirhinal cortex as a function of aging. Graphs illustrate the laminar distribution of calbindin (CB, solid bars), parvalbumin, (PV, open bars), and calretinin (CR, gray bars) in PR from adult, middle-aged, and aged rats.

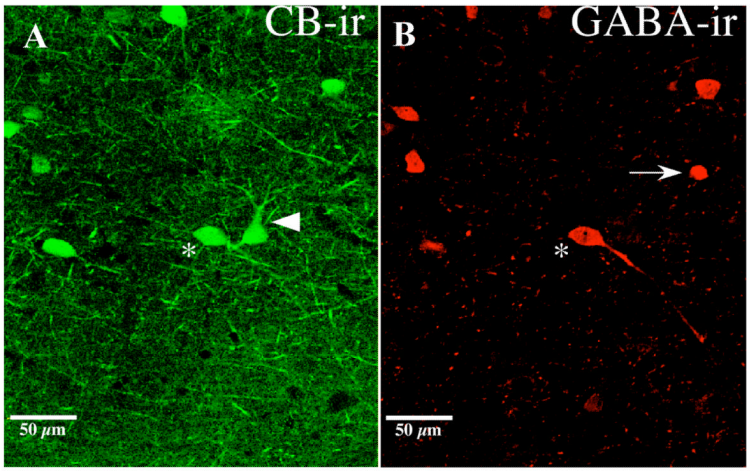

Figure 7.

Double-labeling of calbindin and GABA in rat perirhinal cortex. Confocal laser scanning microscopy (CLSM) of calbindin-labeled (A) and GABA-labeled (B) neurons in layer V of perirhinal cortex (PR) from an aged rat (30 months old). CLSM of PR indicates that not all CB-ir neurons are GABAergic (noted by the large arrow head in part A). A number of CB-immunoreactive neurons were GABAergic (see asterisk in A and B). There were also neurons that were only immunoreactive for GABA, noted by the arrow in part B. The images were collected using a 20X air objective and a digital zoom of 1.5.

Table 1

Relative frequency distribution of calcium binding proteins in adult rat perirhinal cortex

Type of CaBP Immunoreactivity	Layer of Perirhinal Cortex			
	Layer I	Layer II/III	Layer V	Layer VI
CB-ir	0.2 ± 0.1 %	63.6 ± 2.6 % *	28.6 ± 2.2 % *	7.6 ± 0.5 % *
PV-ir	0.6 ± 0.1 %	25.9 ± 1.1 %	61.0 ± 1.1 %	12.5 ± 0.3 %
CR-ir	2.0 ± 0.6 % *	33.5 ± 0.8 %	52.1 ± 1.2 %	12.4 ± 2.4 %

Abbreviations: CB-ir calbindin-immunoreactive; PV-ir parvalbumin-immunoreactive; CR-ir calretinin-immunoreactive. Data were analyzed from 6 slices from each adult rat (CB n = 8; PV n = 6; CR n = 3 rats; age range 3–6 months). For each of the calcium binding proteins, data are expressed as a percentage of the total number of immunoreactive neurons for that calcium binding protein. For each layer, asterisks indicate statistically significant differences relative to the other two groups of calcium binding proteins ($p < 0.005$). For each individual calcium binding protein, the relative frequency of immunoreactive neurons within any layer is significantly different from the relative frequency of immunoreactive neurons in each of the other layers ($p < 0.005$).

Table 2

Calcium binding protein immunoreactivity in rat perirhinal cortex

Calcium Binding Protein	Age Group	Layer of Perirhinal Cortex			
		Layer I	Layer II/III	Layer V	Layer VI
CB-ir	Adult	4 ± 1	2216 ± 388	913 ± 66	248 ± 25
	Middle-Aged	3 ± 1	1361 ± 268	741 ± 63	225 ± 23
	Aged	3 ± 1	1118 ± 239*	689 ± 52*	197 ± 16
PV-ir	Adult	10 ± 2	415 ± 24	983 ± 66	202 ± 17
	Middle-Aged	8 ± 1	359 ± 25	869 ± 80	180 ± 19
	Aged	8 ± 1	348 ± 27	926 ± 80	199 ± 20
CR-ir	Adult	44 ± 19	664 ± 142	1033 ± 225	231 ± 42
	Middle-Aged	44 ± 16	684 ± 146	809 ± 148	197 ± 33
	Aged	44 ± 19	777 ± 211	987 ± 313	181 ± 26

Abbreviations: CB-ir calbindin-immunoreactive; PV-ir parvalbumin-immunoreactive; CR-ir calretinin-immunoreactive. Data were analyzed from 6 slices from each rat (CB n = 8; PV n = 6; CR n = 3 rats) for each age group. Age ranges were as follows: adult (3–6 months), middle-aged (10–12 months), and aged (22–26 months). Asterisks indicate that the number of CB-ir neurons in aged rats was significantly lower in layers II/III and V compared to adults. The number of CB-ir neurons in layers II/III and V of middle-aged rats did not quite reach statistical significance from that of the adults (p = . 06). No statistically significant differences were observed in PV- or CR-ir during aging. Numbers represent the mean ± 1 standard error of the mean.

Table 3

Dual labeling of calbindin and GABA immunoreactivity in rat perirhinal cortex

	Immunoreactivity		
Age Group	**CB-ir**	**GABA-ir**	**CB-ir and GABA-ir**
Adult	155 ± 12	81 ± 15	46 ± 9
Middle-Aged	114 ± 11	95 ± 34	43 ± 2
Aged	92 ± 6 *	71 ± 25	37 ± 11

Abbreviations: CB-ir calbindin-immunoreactive, GABA-ir GABA-immunoreactive. Data were analyzed for 6 slices from each rat (n = 2) from each age group. Age ranges were as follows: adult (3–6 months), middle-aged (10–12 months), and aged (22–26 months). There was a statistically significant effect of age group on the number of CB-ir neurons in perirhinal cortex ($p < 0.05$). Aged rats had significantly fewer CB-ir neurons compared to adult animals, $p < 0.05$. There was no effect of age group on the number of GABA-ir ($p = 0.8$) or double-labeled neurons (CB-ir and GABA-ir; $p = 0.7$). Numbers represent mean ± 1 standard error of the mean.